Ion implantation in titanium dioxide thin films studied by perturbed angular correlations

Juliana Schell, Doru C. Lupascu, Artur Wilson Carbonari, Ronaldo Domingues Mansano, Ibere Souza Ribeiro Junior, Thien Thanh Dang, Irina Anusca, Harsh Trivedi, Karl Johnston, and Reiner Vianden

Citation: Journal of Applied Physics **121**, 145302 (2017); doi: 10.1063/1.4980168
View online: http://dx.doi.org/10.1063/1.4980168
View Table of Contents: http://aip.scitation.org/toc/jap/121/14
Published by the American Institute of Physics

Ion implantation in titanium dioxide thin films studied by perturbed angular correlations

Juliana Schell,[1,2] Doru C. Lupascu,[2] Artur Wilson Carbonari,[3]
Ronaldo Domingues Mansano,[4] Ibere Souza Ribeiro Junior,[3] Thien Thanh Dang,[5]
Irina Anusca,[2] Harsh Trivedi,[2] Karl Johnston,[1] and Reiner Vianden[5]
[1]*European Organization for Nuclear Research (CERN), CH-1211 Geneva, Switzerland*
[2]*Institute for Materials Science and Center for Nanointegration Duisburg-Essen (CENIDE), University of Duisburg-Essen, 45141 Essen, Germany*
[3]*Instituto de Pesquisas Energéticas e Nucleares, Universidade de São Paulo, 05508-000 São Paulo, Brazil*
[4]*Escola Politécnica, Universidade de São Paulo, 05508-010 São Paulo, Brazil*
[5]*Helmholtz-Institut für Strahlen- und Kernphysik, Universität Bonn, 53115 Bonn, Germany*

(Received 14 January 2017; accepted 28 March 2017; published online 13 April 2017)

The local environment in titanium dioxide was studied by the time dependent perturbed γ-γ angular correlation of ^{111}In/^{111}Cd and ^{181}Hf/^{181}Ta at the Helmholtz-Institut für Strahlen-und Kernphysik, Bonn. An introduction to the implantation methodologies performed at the Bonn Radioisotope Separator is presented. The investigation was carried out on thin films, which were deposited by magnetic sputtering on Si. The results show two different sites for both probe nuclei with unique electric quadrupole interaction. Using ^{111}Cd one of them has been attributed to the substitutional Ti at the rutile structure. For ^{181}Ta, the spectra show the anatase phase, with a well-defined electric quadrupole frequency. *Published by AIP Publishing.* [http://dx.doi.org/10.1063/1.4980168]

INTRODUCTION

TiO_2 has a wide range of applications and comparably low production price. It can be used as a photocatalyst for water and air purification, sunscreen material for the protection from UV light, an energy converter in solar cells, white pigment in paints, and for many other applications in the electronics industry.[1–3] It is well known that the electrochemical behavior of doped TiO_2 strongly depends not only on the crystal lattice parameters and the number of oxygen vacancies, but also on the particle size distribution.[4] There is evidence that the grain size determines gas sensing capability and conventional characterizations of TiO_2 films show that Ta doping inhibits growing of grain size.[5] Furthermore, tantalum doping improves the capacity of the photocatalysts to use UV radiation of lower energy.[6] Previous electrical characterization suggests that the n-type behavior of Ta-doped titania layers does not change with the annealing treatment.[7]

The bandgap of Hf-doped TiO_2 is lower than the bandgap of undoped TiO_2[8] while Ta doping leads to significantly enhanced activity in photoelectrochemical water splitting performance.[9] Cd-doped TiO_2 shows higher diffuse reflection under visible light, and lower resistance and band gap values than un-doped TiO_2.[10] Indium doping in TiO_2 can increase the surface area and enlarges the band gap.[11]

Previous TiO_2 Time Differential Perturbed Angular Correlations (TDPAC) or (PAC) measurements were carried out after the addition of ^{181}Hf, ^{111}In, and ^{111m}Cd during the chemical processes of powder sample preparation or by ion implantation in single crystals. Typically, the electric field gradient (EFG) changes according to the type of sample and preparation methods. Wenzel *et al.*[12] performed PAC measurements in pellets at room temperature using the ^{111}In isotope as a function of the annealing temperature and atmosphere. The investigation of the temperature dependence of hyperfine parameters of rutile TiO_2 using the PAC technique was also performed in polycrystalline sample by Adams and Catchen using ^{111}In/Cd and ^{181}Hf/Ta as probe nuclei in the temperature range from 290 K to 1300 K.[13] The authors verified that the axial asymmetry parameter (η) of the EFG decreases from room temperature up to 700 K, the η value essentially vanishes from 700 to 800 K and it increases above 800 K when using ^{111}In/Cd as probe nucleus. A monotonic decrease of the principal EFG component (V_{zz}) was detected with rising temperature. When ^{181}Hf/Ta was used as the probe nucleus, a small variation of η values and slight increase of V_{zz} upon raising temperature was observed. This small variation found by Adams and Catchen was later explained in details by Darriba *et al.* using first principle calculations introducing a thermal expansion coefficient of the TiO_2 lattice. In addition, Darriba *et al.* performed PAC measurements of hyperfine parameters in rutile TiO_2 single crystal using ^{181}Hf/Ta as the probe nuclei as a function of rotation angle and temperature.[14] The experimental values for η and V_{zz} obtained are in agreement with those reported by Adams and Catchen.

Errico *et al.* have also performed PAC measurements in TiO_2 single crystals at room temperature using ^{111}In/Cd as the probe nucleus in addition to the first principle calculations.[15] This study showed that the EFG tensor depends on the charge states, due to different local relaxations that different probe nuclei induce on the host TiO_2 crystal. Furthermore, first principle calculations revealed that a metallic system is formed when a Cd impurity replaces a Ti atom in a super cell, and hence, a change in the symmetry of the electronic charge distribution in the neighborhood is caused.

The phase transition from anatase to rutile was investigated using the TDPAC technique by Banerjee *et al.* and

Das *et al*. using ^{181}Hf/Ta as the probe nucleus in bulk and nanoparticles.[16,17] They determined the hyperfine parameters of TiO_2 using different temperatures and time of annealing. The authors verified a partial phase transition from anatase (5%) to rutile (95%) when the sample was annealed at 823 K for 8 h. In this study the total conversion to rutile phase was verified when the sample was annealed at 1123 K for 4 h, however at the same temperature and when increasing the time of annealing, the anatase phase was detected together with the rutile phase. By annealing at 1223 K for 8 h, the anatase phase was completely converted to rutile indicating the slow kinetics of the phase transition and the growth of the crystallite along with the transfer of the probe nuclide from the surface to bulk. Martucci *et al*.[18] carried out PAC measurements in pellets made by the sol–gel method using ^{181}Hf and ^{111}In as radionuclides. While for ^{111}In just the nuclear quadrupole interaction characteristic for the rutile was obtained, both phases appear in the case of the ^{181}Hf.[18] In our previous work,[19] single crystals were measured after simultaneous implantation of ^{111m}Cd and ^{111}In. For ^{111}In/Cd, the quadrupole frequency was assigned to Cd atoms at the Ti sites at the rutile phase. On the other hand, ^{111m}Cd/Cd behaves completely different under the same implantation and annealing procedures. Furthermore, Banerjee *et al*.[20] using ^{181}Hf did not observe a significant change of the hyperfine parameters of anatase and rutile after exposure to gamma radiation at room temperature, which is an advantage for the use of TiO_2 as immobilizing matrix for nuclear waste.

By measuring as a function of temperature or annealing, all previous works report a strong temperature dependence of the hyperfine parameters. Errico *et al*.[21] used Full-Potential Linearized-Augmented Plane Waves (FLAPW) calculations in order to explain the temperature dependence EFG tensor in TIO_2 with Cd impurities. The theoretical calculations showed that the temperature dependence of the EFG tensor arise from the electronic structure of Cd, which induces structural relaxations which are dependent on the expansion of the structure.

Here, we present results as a function of measurement temperature of thin films after the implantation of ^{181}Hf and ^{111}In. To our knowledge, such measurements have never been done before. Our results are discussed based upon the predictions of previous first principle calculations and compared with polycrystals and pellets measurements. Table I summarizes the experimental hyperfine parameters from previous experimental results obtained for both probes in bulk rutile and anatase phases. There is a fundamental interest in comparing experiments performed with thin films and pellets, since the number of oxygen vacancies differs significantly with clear consequences for the electrical properties. The lattice distortions lead to changes of the electric field gradients at the probe lattice site which can be measured by the PAC technique. This allows us to follow the evolution of defect recovery and of phase transitions as a function of annealing and/or measuring temperature with high resolution on a local scale, and a sensitivity far above the capabilities of traditional diffraction or macroscopic techniques.

Perturbed angular correlations

The time differential PAC technique is a well-established method to characterize the environment of local probe isotopes in solids using a cascade of gamma-rays emitted by the probe nucleus. It allows the measurement of electromagnetic fields by hyperfine interaction with radioactive probe nuclei with very small concentrations of the probe and relatively short half-life.[24] Typically, using just 10^{12} atoms of the impurity probe, no essential alteration occurs in the system under investigation. During time (t) in which the PAC isotope remains in the intermediate state between the two gamma rays, the nucleus is subject to a hyperfine interaction, which promotes a change in the occupation of the different sublevels. Therefore, the probability of emission of the second gamma in a given direction is time modulated. Considering the property where the photon angular momentum is always co-linear to its direction of propagation, the first gamma ray γ_1 causes a preferential orientation of the spin I regarding the course of propagation called nuclear spin alignment. To detect this alignment, the emission of the second gamma ray is needed. The perturbed angular correlation function is given by the γ_1–γ_2 cascade anisotropy terms, $A_{k\gamma 1}$ and $A_{k\gamma 2}$, the perturbation factor $G_{22}(t)$ and the Legendre polynomials $P_k \cos\theta$ and has the following form:

TABLE I. Hyperfine parameters from previous experimental results. For the V_{zz} calculation, we used the old quadrupole moment value of 0.83(13) b[22] for ^{111}In(^{111}Cd). However, the current one is 0.683(20) b.[23]

^{181}Hf/^{181}Ta				^{111}In/^{111}Cd			
η	V_{zz} (10^{21} V/m^2)	Assigned structure	Reference	η	V_{zz} (10^{21} V/m^2)	Assigned structure	Reference
0.56 (1)	13.65 (10)	Rutile	17	0.18 (1)	5.34 (1)	Rutile	13
0.22 (1)	4.62 (1)	Anatase	17	0.18 (1)	5.23 (5)	Rutile	12
0.57 (1)	13.41 (02)	Rutile	20	0.18 (1)	5.34 (1)	Rutile	21
0.23 (1)	4.64 (2)	Anatase	20	…	5.28	…	18
…	14.3 (4)	…	18	…	9.95	…	18
…	8.4 (2)	…	18	0.18 (1)	5.23 (1.2)	Rutile	19
0.22 (1)	4.93 (1)	Anatase	16				
0.62 (7)	8.68 (2)	Unknown	16				
0.56 (1)	14.6 (4)	Rutile	16				

$$W(\theta, t) = \sum_{k=0}^{k=k_{máx}} A_{kk} G_{kk}(t) P_k \cos\theta. \quad (1)$$

The spectra are histograms of events which represent pairs γ_1 and γ_2 originated from the same nucleus and correspond to a set time interval in accordance with the calibration time between two MCA neighboring channels. The accidental coincidences are from γ_1–γ_2 pairs not emitted by the same nucleus, and their rate depends on the activity of the sample. After subtraction of accidental coincidences one can obtain the perturbation function given by

$$R(t) = A_{kk} G_{kk}(t) = 2 \cdot \left(\frac{W(180°, t) - W(90°, t)}{W(180°, t) + 2W(90°, t)} \right). \quad (2)$$

The theoretical equation that defines the perturbation factor $G_{22}(t)$ takes on different shapes according to the type of hyperfine interaction. For quadrupole interactions of the nuclear spin $I = \frac{5}{2}$, only three transition frequencies are obtained $\omega_0 = \omega_1$, $2\omega_0 = \omega_2$, and $3\omega_0 = \omega_3$, as it follows the equation

$$G_{22}(t) = \frac{1}{5} \left(1 + \frac{13}{7} \cos\omega_0 t + \frac{10}{7} \cos 2\omega_0 t + \frac{5}{7} \cos 3\omega_0 t \right). \quad (3)$$

The fraction f of each crystalline site occupied by the PAC probe is calculated taking into consideration the following equation:

$$R(t) = A_{22} G_{22}(t) = A_{22} \sum_i f_i G_{22}^i(t). \quad (4)$$

The electric field gradient components V_{xx}, V_{yy}, and V_{zz} are associated and represented by the asymmetry parameter $\eta = (V_{xx} - V_{yy})/V_{zz}$. It describes the asymmetry of the EFG tensor and is obtained from the ratio ω_2/ω_1 which varies between 2 and 1 for $0 \leq \eta \leq 1$.

EXPERIMENTAL

Implantation at BONIS, the Bonn Radioisotope Separator

The room temperature ^{181}Hf and ^{111}In implantations were performed at the Bonn Radioisotope Separator (BONIS) located at Helmholtz-Institut für Strahlen-und Kernphysik (HISKP), which is an ion implanter used for the investigation of materials. Since about 50 years, a wide variety of ions (stable or radioactive) have been accelerated, separated, and implanted at BONIS.[25]

Furthermore, BONIS stands out by its possibility to accelerate ions within a wide range of energies, from 0.5 to 160 keV, making it possible to investigate material properties from the surface to depths of several tens of nanometers. Next to the BONIS building is a cyclotron, which provides radioisotopes that can be used in the implantations. The 160 keV implantation of ^{111}In was carried out using a liquid solution of commercially available $^{111}InCl_3$. First of all, 15 μl of this solution were pipetted into the graphite heater and evaporated to dryness so that just $^{111}InCl_3$ salt remains, and this step was carried out twice. Subsequently, a small amount of stable $InCl_3$ powder was added into the graphite heater in order to get a stable line in the mass spectrum. Then, the graphite heater was coupled to the oven. Finally, the oven was connected to the ion source. After evacuation, the $InCl_3$ was heated in the ion source in order to start the process of sublimation, dissociation, and ionization of the ^{111}In. It crosses the ionization chamber, which is formed by a cathode and an anode. The ionized elements were extracted from the ionization chamber and then focused and accelerated up to an energy of 80 keV. The mass separation was achieved by applying a magnetic field perpendicular to the beam in a 55° sector. A Faraday cup and a probe oscillator were used to control the intensity of the ion fluxes that are implanted. Up to 5 samples can be mounted on the sample holder to be implanted; thus, it is not necessary to break the system vacuum after each implantation. In order to get a homogenous implantation, the ion beam could be swept over the sample by the use of x-y capacitors. A different technique was used for the 80 keV implantation of ^{181}Hf. Here, natural HfO_2 was neutron irradiated in order to produce ^{181}Hf via the ^{180}Hf(n,γ)^{181}Hf reaction. Since HfO_2 is very stable after being inserted into the ion source, CCl_4 was added in order to dissociate HfO_2 forming Hf^+ ions in the heating process. The amount of implanted ions was lower than 10^{12} atoms/cm^2.

The thin films were deposited by sputtering on Si (100) p-type wafer. The custom-made 4-detector PAC spectrometer was equipped with BaF_2 detectors. Following the implantation, rapid thermal annealing (RTA) and measurements were performed in vacuum (10^{-6} mbar). The theoretical perturbation function was fitted to the spectra using the *Nightmare*[26] software to extract the hyperfine parameters.

After the PAC measurements, Atomic Force Microscopy (AFM) images of the films were acquired using a commercial AFM set-up (MFP3D, Asylum Research). A sharp-tip cantilever (Nanosensors PPP-SEIHR; radius ~10 nm) was used for imaging. The topography images were acquired in a closed loop contact mode, and the displayed images correspond to the height trace.

RESULTS AND DISCUSSION

The PAC spectra from Figures 1 and 2 display a superposition of two quadrupole interaction signals. Figures 3 and 4 display the temperature dependence of the hyperfine parameters obtained from the fit, also shown in Tables II and III. To help the discussion, the graphics have been separated into zones (A, B, or C) defined by the shaded areas. The sites 1 or 2 are distinguished by EFG_1/EFG_1' and EFG_2/EFG_2'. In the case of ^{111}Cd, only the rutile structure was present in both environments. Both are usually assigned to the Cd at the substitutional Ti site, with one of them under a higher degree of disorder around the Cd probe.

Since the RTA was performed at 873 K, the amplitude of the spectrum and hyperfine parameters change drastically when measuring at 923 K using ^{111}In(^{111}Cd). This is a fingerprint of a dependence on the history of thermal treatments,

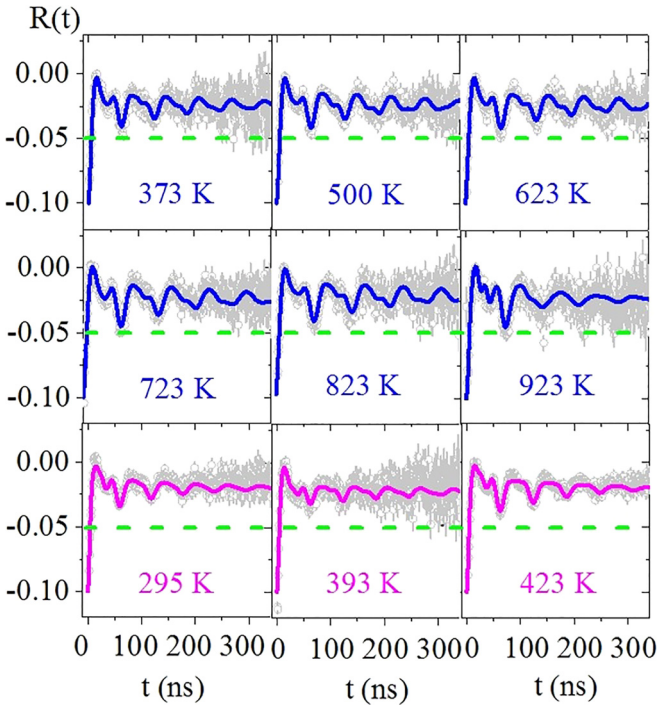

FIG. 1. PAC spectra of TiO_2 thin films measured using $^{111}In(^{111}Cd)$ as probe nuclei after RTA at 873 K for 10 min in vacuum. The three spectra in the bottom row were measured after measurement at 923 K. The least-squares fits of the hyperfine parameters are represented by the blue and magenta solid curves.

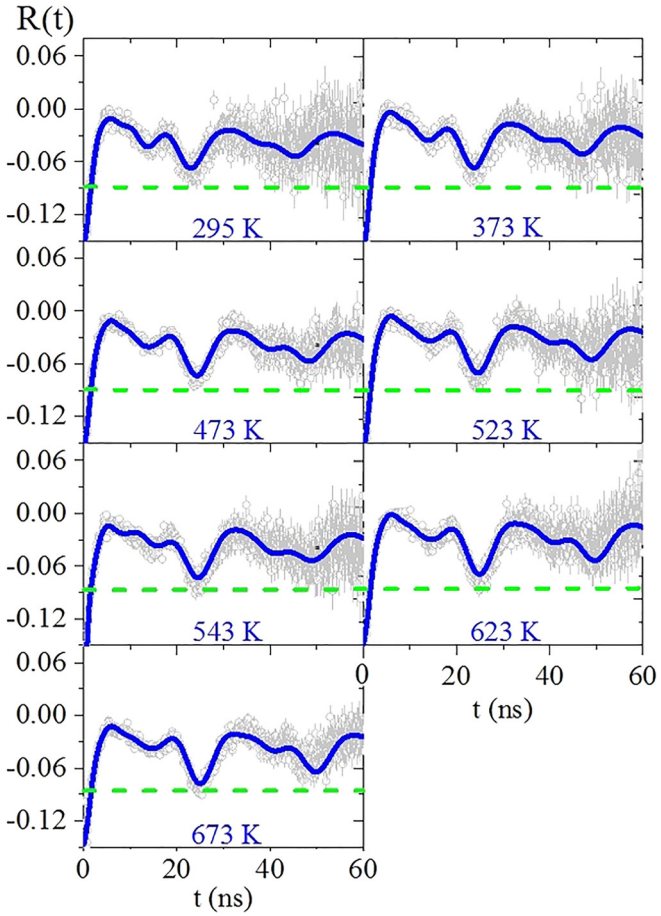

FIG. 2. PAC spectra of the TiO_2 thin film measured using $^{181}Hf(^{181}Ta)$ as probe nuclei after RTA performed at 1073 K during 10 min in vacuum. The least-squares fits of the hyperfine parameters are represented by the blue solid curves. The order of the spectra corresponds to the measurement sequence.

specially noted by measuring again at room temperature. This effect is apparent in the spectra as a damping of R(t) better seen with the magenta solid line. The subsequent spectra, at 393 K and 423 K, show a gradual recovery of the amplitude. A slow $^{111}In(^{111}Cd)$ diffusion process can be related to the observed effect due to the dynamic character of the perturbed angular correlation.[27] Moreover, the small oxygen deficit that is expected under vacuum conditions strongly enhances the diffusion.[12] There is no complete structural phase transformation observable under the measurement conditions. Site 1 presents values close to a rutile cell in a charged state.[14,15,21] As expected, it shows monotonic and less strong temperature dependence. In particular, in zone A, the asymmetry is $\eta \sim 0$ and was obtained after the measurement at higher temperatures. It changes to $\eta \sim 1$ from 373 K on. Over the temperature range, the probe at site 2 presents strong temperature dependence of the quadrupole frequencies. This effect is attributed to lattice distortions due to the larger ionic radius of Cd at the Ti substitutional site.

At zones B and C of Figure 3, the fraction of site 2 decreases slightly, remaining the main interaction.

On the other hand, the PAC spectra for $^{181}Hf/Ta$ show the anatase phase characterized by pure static quadrupole interaction for the site 1. It is noticeable that the spectra amplitude does not change by increasing the measurement temperature. This probe nucleus is not as sensitive as $^{111}In/Cd$ to variations in the Fermi level of the material. The hyperfine parameters show dependence on the temperature, but no evidence of directional dynamic interaction effects. One interaction presents a well-defined electric quadrupole frequency, $\delta < 6\%$, and an asymmetry parameter $\eta \sim 0.22$, corresponding to $\omega_0 = 270\,\text{Mrad/s}$ with monotonic temperature dependence. This interaction has been attributed to the anatase phase.[16,17,20]

For comparison, for the V_{zz} calculation, we used the former quadrupole moment value of 2.35(6) b[28] for $^{181}Hf/^{181}Ta$.

The other interaction is characterized by an electric quadrupole frequency that varies from 455 to 480 Mrad/s, which can be assigned to defects and has also been observed by Banerjee *et al.*[16] and Martucci.[18] It increases up to 473 K, in zone A, and is more widely distributed, $\delta > 15\,\%$, with the axial asymmetry parameter $\eta \sim 0$. In zone B, the quadrupole frequency reduces and remains stable in zone C. Interestingly, the rapid thermal annealing at high temperature, 1073 K, could not induce a major fraction for the rutile in thin films. This means that the phase transformation occurs at even higher temperature in the same way that it occurs in bulk and nanoparticle samples.[13,16,17]

Figure 5 displays the AFM topography images and their Fast-Fourier analysis for the TiO_2/Ta and the TiO_2/Cd films showing distinct peaks, suggesting the central grain size lying around 400 nm and 285 nm, respectively. This might confirm the evidence that Ta doping inhibits grain size growing.[5] However, a visual inspection suggests a weakly

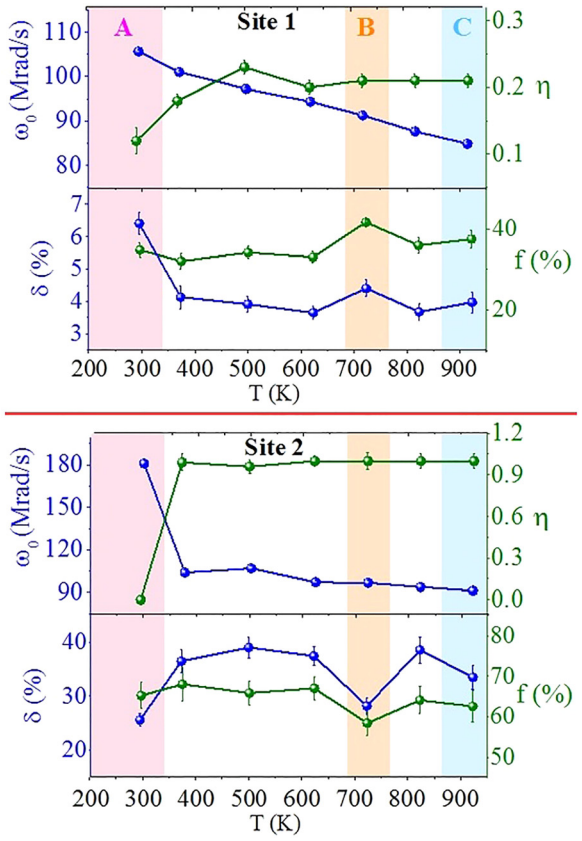

FIG. 3. Hyperfine parameters and their respective errors in the TiO_2 thin film using $^{111}In(^{111}Cd)$ as the test nucleus. The measurements highlighted in zone A were not taken following an ascending order of temperature. Some error bars cannot be seen, because their uncertainties are smaller than the data points.

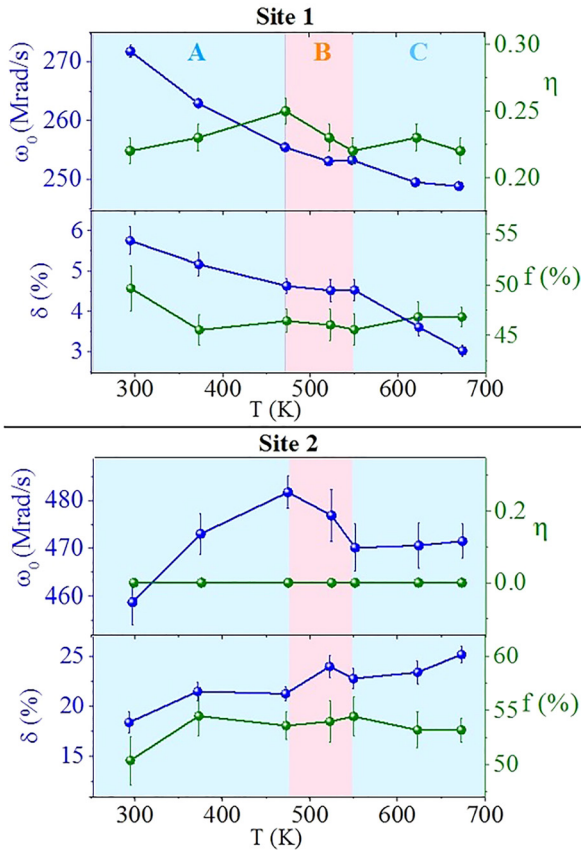

FIG. 4. Hyperfine parameters and their respective errors in the TiO_2 thin film using $^{181}Hf(^{181}Ta)$ as the test nucleus. Some error bars cannot be seen, because their uncertainties are smaller than the data points.

observable finer grain structure, with the grain sizes ranging down to 100 nm.

CONCLUSIONS

We presented the hyperfine analysis of TiO_2 thin films by means of PAC spectroscopy as a function of temperature. A high percentage of ^{181}Hf or ^{111}In could substitute Ti after RTA at 1073 K and 873 K, respectively. The behavior of the observed nuclear quadrupole interaction for ^{111}Cd or ^{181}Ta atoms is dependent on sample type for thin films as well as pellets at the non-distorted substitutional site. In contrast, thin films measured with ^{111}Cd presented a second quadrupole interaction, named site 2, which undergoes drastic changes, since defects change strongly due to temperature changes in thin films. Using ^{111}Cd uniquely the rutile structure was observed. On the other hand for ^{181}Ta, the PAC spectra clearly show the anatase phase, probably indicating that the Hf implantation induces a local structural change of TiO_2. This result is promising; therefore, new measurements are foreseen via Rutherford backscattering spectrometry and nuclear magnetic resonance using Ti probes.

The results shown in this work are part of Ph.D. thesis[29] and were presented as oral presentations at the ISOLDE Workshop and Users meeting 2012 and 2014 that was held at CERN, Switzerland, and at EXMATEC 2016, in Aveiro, Portugal. In addition a poster presentation took place at the *DPG Spring Meeting of the Condensed Matter Section*

TABLE II. Hyperfine parameters from $^{111}In/^{111}Cd$ experimental results.

	Site 1				Site 2			
Temperature (K)	η	V_{zz} (10^{21} V/m^2)	δ (%)	f (%)	η	V_{zz} (10^{21} V/m^2)	δ (%)	f (%)
295	0.12 (2)	5.6 (1)	6.41 (3)	34.78 (2)	0	9.6 (2)	25.55 (1)	65.22 (3)
373	0.18 (1)	5.3 (1)	4.14 (3)	32 (2)	0.99 (6)	5.5 (1)	36.5 (2)	68 (4)
500	0.23 (1)	5.1 (1)	3.92 (2)	34.15 (2)	0.96 (5)	5.7 (1)	39.03 (2)	65.85 (3)
623	0.20 (1)	5.0 (1)	3.66 (2)	33.02 (1)	1.00 (4)	5.1 (1)	37.44 (2)	67 (3)
723	0.21 (1)	4.8 (1)	4.41 (3)	41.6 (1)	1.00 (6)	5.1 (1)	28.17 (2)	58.4 (3)
823	0.21 (1)	4.6 (1)	3.68 (3)	35.92 (2)	1.00 (5)	5.0 (1)	38.55 (2)	64.08 (4)
923	0.21 (1)	4.5 (1)	3.98 (3)	37.45 (2)	1.00 (5)	4.8 (1)	33.5 (2)	62.55 (4)

TABLE III. Hyperfine parameters from ^{181}Hf/^{181}Ta experimental results.

	Site 1				Site 2			
Temperature (K)	η	V_{zz} (10^{21} V/m^2)	δ (%)	f (%)	η (fixed)	V_{zz} (10^{21} V/m^2)	δ (%)	f (%)
295	0.22 (1)	5.1 (1)	5.75 (3)	49.66 (2)	0	8.5 (2)	18.38 (2)	50.34 (2)
373	0.23 (1)	4.9 (1)	5.17 (3)	45.53 (1)	0	8.8 (2)	21.47 (2)	54.47 (2)
473	0.25 (1)	4.8 (1)	4.63 (2)	46.43 (2)	0	9.0 (2)	21.24 (1)	53.57 (1)
523	0.23 (2)	4.7 (1)	4.52 (3)	46.04 (2)	0	8.9 (2)	23.94 (2)	53.96 (2)
550	0.22 (1)	4.7 (1)	4.53 (3)	45.57 (2)	0	8.7 (2)	22.74 (2)	54.43 (2)
623	0.23 (1)	4.6 (1)	3.61 (2)	46.83 (2)	0	8.7 (2)	23.37 (2)	53.17 (2)
673	0.22 (1)	4.6 (1)	3.02 (3)	46.83 (1)	0	8.8 (2)	25.14 (1)	53.17 (1)

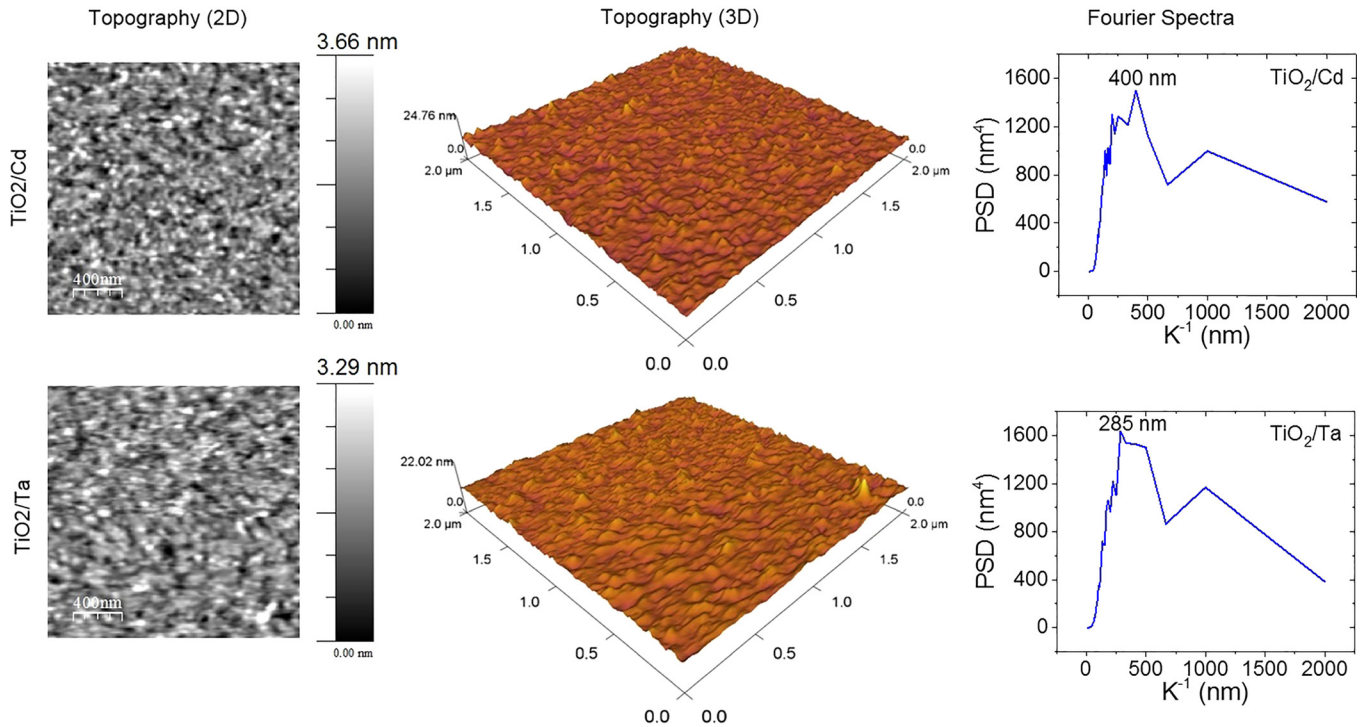

FIG. 5. AFM topography images and their fast-Fourier analysis for the TiO_2/Ta and TiO_2/Cd films.

(SKM) that was held at the University of Regensburg in 2013, Germany.

ACKNOWLEDGMENTS

The research has received funding from the Federal Ministry of Education and Research (BMBF) through Grant Nos. 05K13TSA and 05K16PGA and DAAD/CNPq through Grant No. 290102/2011-1. We are thankful to Ms. Noll and the BONIS team at HISKP, Bonn, for the implantations and the warm hospitality. Language corrections provided by Ms. J. Weterings were greatly appreciated. Dr. J. G. Martins Correia is thankfully acknowledged for great discussions about the PAC technique.

[1]H. Chen, Z. Wei, K. Yan, Y. Bai, and S. Yang, J. Phys. Chem. Lett. **5**, 2890 (2014).
[2]W. Choi, A. Termin, and M. R. Hoffmann, J. Phys. Chem. **98**, 13669 (1994).
[3]M. Cargnello, T. R. Gordon, and C. B. Murray, Chem. Rev. **114**, 9319 (2014).
[4]V. V. Zheleznov, E. I. Voit, Y. V. Sushkov, S. A. Sarin, V. G. Kuryavyi, D. P. Opra, S. V. Gnedenkov, S. L. Sinebryukhov, and A. A. Sokolov, IOP Conf. Ser.: Mater. Sci. Eng. **112**, 012016 (2016).
[5]N. Bonini, M. C. Carotta, A. Chiorino, V. Guidi, C. Malagu, G. Martinelli, L. Paglialonga, and M. Sacerdoti, Sens. Actuators, B **68**, 274 (2000).
[6]C. M. Visinescu, R. Sanjines, F. Levy, V. Marcu, and V. I. Parvulescu, J. Photochem. Photobiol., A **174**, 106 (2005).
[7]E. Comini, M. Ferroni, V. Guidi, A. Vomiero, P. G. Merli, V. Morandi, M. Sacerdoti, G. Della Mea, and G. Sberveglieri, Sens. Actuators, B **108**, 21 (2005).
[8]L. Lezhong, Y. Weiqing, D. Yingchun, and Z. Xinghua, J. Semicond. **33**, 012002 (2012).
[9]M. Altomare, K. Lee, M. S. Killian, E. Selli, and P. Schmuki, Chem.-Eur. J. **19**, 5841 (2013).
[10]Y. Li, Y. Guo, Y. Li, and X. Zhou, Electrochim. Acta **200**, 29–36 (2016).
[11]M. Tahir and N. S. Amin, Appl. Catal., B **162**, 98 (2015).
[12]T. Wenzel, A. Bartos, K. P. Lieb, M. Uhrmacher, and D. Wiarda, Ann. Phys. **504**, 155 (1992).
[13]J. M. Adams and G. L. Catchen, Phys. Rev. B **50**, 1264 (1994).
[14]G. N. Darriba, L. A. Errico, P. D. Evercheim, G. Fabricius, and M. Renteria, Phys. Rev. B **79**, 115213 (2009).
[15]L. A. Errico, G. Fabricius, M. Renteria, P. de La Presa, and M. Forker, Phys. Rev. Lett. **89**, 055503 (2002).
[16]D. Banerjee, S. K. Das, S. V. Thakare, P. Y. Nabhiraj, R. Menon, R. K. Bhandari, and K. Krishnan, J. Phys. Chem. Solids **71**, 983 (2010).

[17]S. K. Das, S. V. Takhare, and T. Butz, J. Phys. Chem. Solids **70**, 778 (2009).
[18]T. Martucci, J. M. Ramos, A. W. Carbonari, A. S. Silva, and R. N. Saxena, *International Nuclear Atlantic Conference* (Associação Brasileira de Energia Nuclear, 2011), ISBN: 978-85-99141-04-5.
[19]J. Schell, D. C. Lupascu, J. G. M. Correia, A. W. Carbonari, M. Deicher, M. B. Barbosa, R. D. Mansano, K. Johnston, I. S. Ribeiro, Jr., and ISOLDE Collaboration, Hyperfine Interact. **238**(2) (2016).
[20]D. Banerjee, R. Guin, S. K. Das, and S. V. Thakare, J. Radioanal. Nucl. Chem. **290**, 119 (2011).
[21]L. Errico, Hyperfine Interact. **158**, 29 (2004).
[22]P. Herzog, K. Freitag, M. Reuschenbach, and H. Walitzki, Z. Phys. A: At. Nucl. **294**, 13 (1980).
[23]H. Haas, M. B. Barbosa, and J. G. Correia, Hyperfine Interact. **237**, 115 (2016).
[24]A. Abragam and R. V. Pound, Phys. Rev. **92**, 943 (1953).
[25]K. Freitag, Radiat. Eff. **44**, 185 (1979).
[26]Nightmare (MDI) Version RC 3 (1.2.0.247). Copyright (2005–2010) from the group Reiner Vianden and (2008–2010) Ronan Nédélec, Bonn University.
[27]D. Lupascu, S. Habenicht, K.-P. Lieb, M. Neubauer, M. Uhrmacher, and T. Wenzel, Phys. Rev. B **54**, 871 (1996).
[28]S. Wu, Nucl. Data Sheets **106**, 367 (2005).
[29]J. Schell, "Investigation of hyperfine parameters in pure and 3d transition metal doped SnO_2 and TiO_2 by means of perturbed gamma-gamma angular correlation spectroscopy," Ph.D. thesis, São Paulo University, Brazil, 2015.